Precision Engineering 38 (2014) 409–413

Contents lists available at ScienceDirect

Precision Engineering

journal homepage: www.elsevier.com/locate/precision

Phase correction for frequency response function measurements

Vasishta Ganguly, Tony L. Schmitz*

University of North Carolina at Charlotte, Charlotte, NC, United States

ARTICLE INFO

Article history:
Received 17 April 2013
Received in revised form 31 October 2013
Accepted 17 December 2013
Available online 25 December 2013

Keywords:
Namics
Modal
Time delay
Accelerometer
Capacitive sensor

ABSTRACT

In modal testing, an impulse is often used to excite the structure and a linear transducer is used to measure the response. For these impact tests, two signals are measured: the impulsive force and the vibration response. Any lack of synchronization in the time domain acquisition of the two signals results in a frequency-dependent phase error in the frequency response function, or FRF. However, knowledge of the time delay may be used to correct the corresponding phase error. In this research, tests were conducted to measure the frequency-dependent phase error for a capacitive sensor and a frequency domain technique is proposed to correct the FRF. The method was validated using an FRF measurement of a cylindrical artifact mounted in a milling machine spindle.

1. Introduction

It is often necessary to identify the vibration response of structures. Examples include bridges, automobiles, machine tools, and measuring instruments. The vibration characteristics of these structures are traditionally described using the frequency response function, or FRF. This complex-valued function defines the vibration output to force input ratio in the frequency domain [1]. It represents the steady-state (particular) solution to the system differential equation of motion. In the following paragraphs, the FRF is derived and then the influence of a time delay in the response measurement on the FRF phase is described.

1.1. FRF definition

For a lumped parameter[1] single degree of freedom spring-mass-damper system with a harmonic force input, the timedomain equation of motion is:

$$m\ddot{x} + c\dot{x} + kx = Fe^{i\omega t}, \tag{1}$$

where m is the mass, c is the viscous damping coefficient, k is the stiffness, and $f(t) = Fe^{i\omega t}$ is the force (ω is the forcing frequency in rad/s). Also, $x(t)$ is the displacement, $\dot{x}(t)$ is the velocity, and $\ddot{x}(t)$ is the acceleration.

The total solution to the forced vibration equation of motion (Eq. (1)) has two parts: the homogeneous, or transient, solution; and the particular, or steady-state, solution. The steady-state portion remains after the transient has attenuated and it persists as long as the force is acting on the system. The particular solution takes the same form as the forcing function. The resulting vibration has the same frequency as the harmonic force. Specifically, given the force $f(t) = Fe^{i\omega t}$, the corresponding steady-state response can be written as $x(t) = Xe^{i\omega t}$. Given this form for the position, the velocity is $\dot{x}(t) = i\omega Xe^{i\omega t}$ and the acceleration is $\ddot{x}(t) = (i\omega)^2 Xe^{i\omega t} = -\omega^2 Xe^{i\omega t}$. Substituting these expressions in Eq. (1) gives:

$$(-m\omega^2 + i\omega c + k)Xe^{i\omega t} = Fe^{i\omega t}. \tag{2}$$

Eq. (2) relates the force to the resulting vibration as a function of the forcing frequency, ω. Rewriting gives the ratio of the output (the complex-valued vibration, X) to the input (the real-valued force, F); this is the FRF for the system [2].

$$\frac{X}{F}(\omega) = \frac{1}{-m\omega^2 + i\omega c + k} \tag{3}$$

Eq. (3) can be rewritten using the frequency ratio, $r = \omega/\omega_n$, where $\omega_n = \sqrt{k/m}$ (rad/s) is the (undamped) natural frequency, and dimensionless damping ratio, $\zeta = c/2\sqrt{km}$; see Eq. (4). The FRF is typically represented as either the real, $Re(X/F(r))$, and imaginary, $Im(X/F(r))$, parts or, alternately, the magnitude, $|X/F(r)|$, and phase, $\phi(r)$. See Eqs. (5)–(8).

$$\frac{X}{F}(r) = \frac{1}{k}\left(\frac{1}{(1-r^2)+i2\zeta r}\right) = \frac{1}{k}\left(\frac{(1-r^2)-i2\zeta r}{(1-r^2)^2+(2\zeta r)^2}\right) \tag{4}$$

* Corresponding author. Tel.: +1 117046875086.
E-mail address: tony.schmitz@uncc.edu (T.L. Schmitz).

[1] In a lumped parameter system, the mass is concentrated at the coordinate that describes the system motion and the spring and damper are assumed to be massless.

0141-6359/$ – see front matter © 2013 Elsevier Inc. All rights reserved.
http://dx.doi.org/10.1016/j.precisioneng.2013.12.007

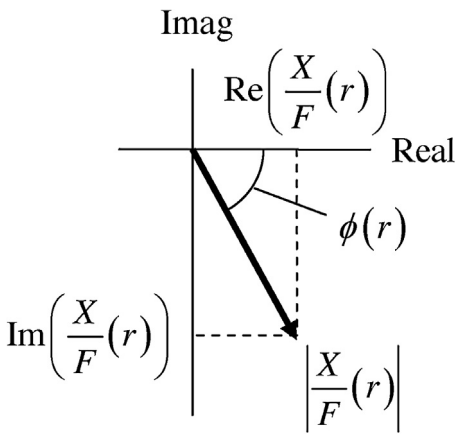

Fig. 1. Vector description of the relationships between the real/imaginary parts and magnitude/phase. The phase indicates the complex displacement lag relative to the force (real-valued and pointing to the right along the real axis).

$$Re\left(\frac{X}{F}(r)\right) = \frac{1}{k}\left(\frac{(1-r^2)}{(1-r^2)^2+(2\zeta r)^2}\right) \tag{5}$$

$$Im\left(\frac{X}{F}(r)\right) = \frac{1}{k}\left(\frac{-2\zeta r}{(1-r^2)^2+(2\zeta r)^2}\right) \tag{6}$$

$$\begin{aligned}\left|\frac{X}{F}(r)\right| &= \sqrt{\left(Re\left(\frac{X}{F}(r)\right)\right)^2+\left(Im\left(\frac{X}{F}(r)\right)\right)^2} \\ &= \frac{1}{k}\sqrt{\frac{1}{(1-r^2)^2+(2\zeta r)^2}}\end{aligned} \tag{7}$$

$$\phi(r) = \tan^{-1}\left(\frac{Im(X/F(r))}{Re(X/F(r))}\right) = \tan^{-1}\left(\frac{-2\zeta r}{1-r^2}\right) \tag{8}$$

The relationships between the real/imaginary parts and the magnitude/phase are conveniently defined in the complex plane as shown in Fig. 1. Based on this vector representation of the FRF at a particular r value, it is seen that a phase error will affect both the Re and Im values.

1.2. Time delay

Next, consider the effect of a time delay between the actual system response and the measured vibration. This can be introduced, for example, by the amplifying/signal conditioning electronics that convert the transducer output to the voltage that is subsequently sampled and converted from the timedomain to the frequency domain for the FRF computation. As shown schematically in Fig. 2, the measurement signal may be time delayed by a small amount relative to the actual vibration. For a constant time delay, this yields a phase error that increases linearly with frequency. Fig. 3 displays the actual, x_a, and measured, x_m, signals for a 50 ms time delay at three different oscillating frequencies, f, of {1, 2, and 3} Hz. The corresponding phase errors are {−18, −36, and −54} deg. The phase error was calculated using Eq. (9).

$$\Delta\phi(f) = \cos^{-1}\left(\frac{x_a x_m}{|x_a||x_m|}\right) \tag{9}$$

Using Eq. (9), the frequency-dependent phase error can be calculated for any time delay between x_a and x_m. Fig. 4 shows the linearly-varying phase error for a range of time delays from 10 μs to 100 μs. The slope for each linear trend is listed in the legend. It is seen that a 50 μs delay gives a slope of −18 deg/kHz and, therefore, a −90 deg phase error at 5000 Hz. Using Fig. 1, it is observed

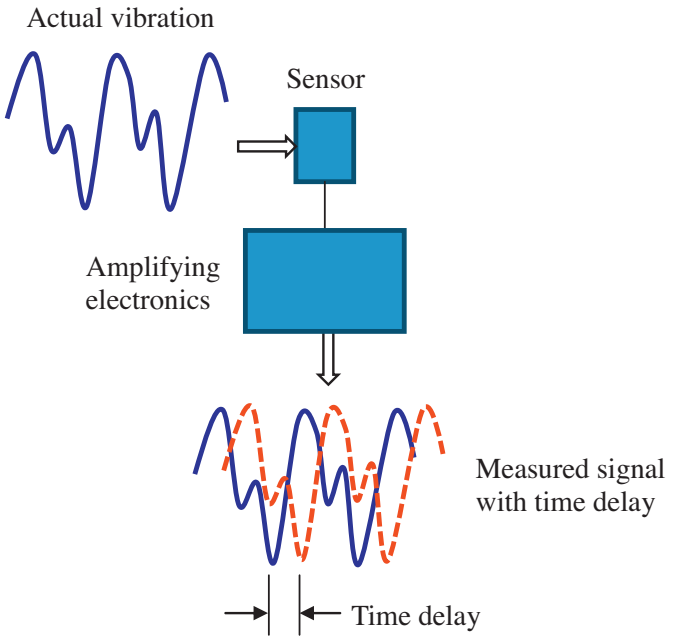

Fig. 2. Representation of a time delay between the actual (solid line) and measured (dotted line) vibration signals.

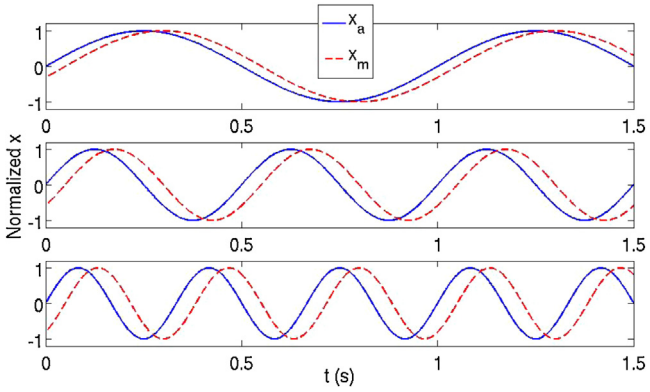

Fig. 3. Effect of 50 ms time delay on phase: (top) 1 Hz frequency gives a −18 deg phase lag; (middle) 2 Hz frequency gives a −36 deg phase lag; and (bottom) 3 Hz frequency gives a −54 deg phase lag.

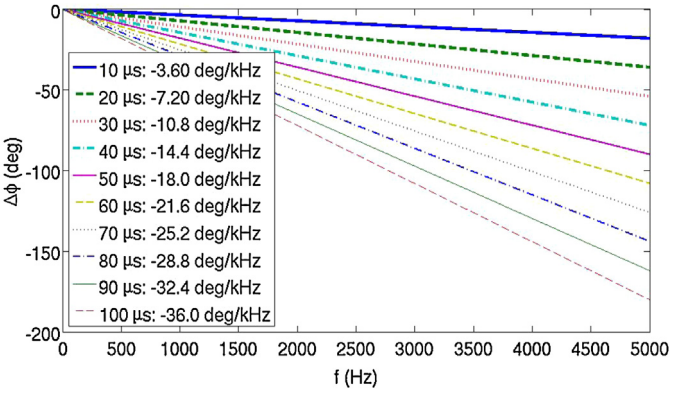

Fig. 4. Frequency-dependent phase error, $\Delta\phi$, as a function of frequency, f. The linear trends for time delays from {10 to 100} μs are displayed.

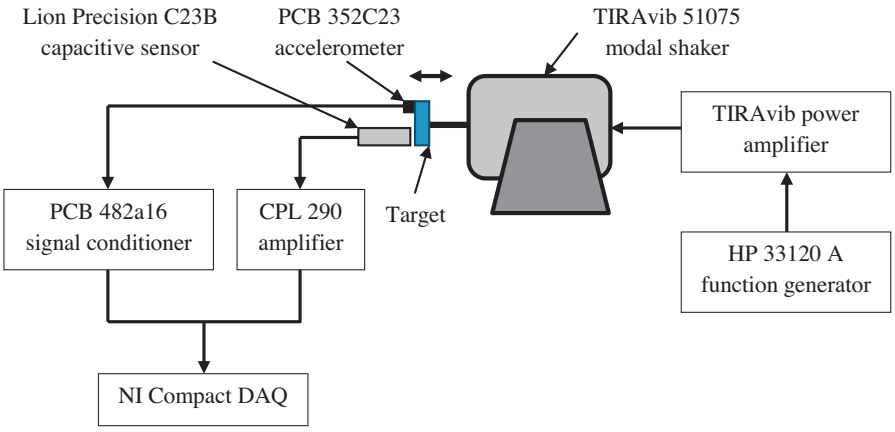

Fig. 5. Experimental setup.

that a −90 deg phase error switches the amplitudes of the real and imaginary parts and changes the sign of the imaginary part.

2. Background

The basic hardware required to measure FRFs includes: a mechanism for known force input across the desired frequency range (or bandwidth); a transducer for vibration measurement, again with the required bandwidth; and a dynamic signal analyzer to record the time-domain force and vibration inputs and convert these into the desired FRF. This conversion includes calculating the Fourier transform of the inputs and then computing their complex ratio. The FRF may be expressed as: receptance/compliance, the ratio of displacement to force; mobility, the ratio of velocity to force; or accelerance/inertance, the ratio of acceleration to force, depending on the selected transducer [2].

There are three common types of force excitation. These include: fixed frequency sine wave, where the FRF is determined one frequency at a time by applying a sinusoidal force at each frequency within the desired bandwidth; random signal, where the frequency content of the random signal may be broadband (white noise) or truncated to a limited range (pink noise) and the response is averaged over a selected time interval; and impulse, where a short duration impact is used to excite the structure over a broad frequency range and the corresponding response is measured. To generate these known excitation forces, two common types of force input hardware are applied:shaker, which includes a harmonically driven armature actuated along its axis by a magnetic coil or hydraulic force, and a base; and impact hammer, which incorporates a force transducer located at a metal, plastic, or rubber tip to measure the force input during a hammer strike. When a hammer is used in conjunction with a vibration transducer, the measurement procedure is referred to as impact testing.

Vibration transducers are available in both non-contact and contact types. While non-contact transducers, such as capacitive sensors and laser vibrometers, may be preferred because they do not influence the system dynamics (by adding mass), contacting types, such as accelerometers, are often more convenient to implement. As a compromise, low mass accelerometers may be used to minimize the influence on the test structure. They are attached at the location of interest using wax, adhesive, a magnet, or a threaded stud and then removed when the testing is completed. In this study, both a capacitive sensor and a piezoelectric accelerometer were used. Brief descriptions of each are included here for completeness.

Noncontact capacitive sensors measure changes in capacitance, the ability of a body to hold an electrical charge. When a voltage is applied to two conductors separated by some distance, an electric field is produced between them and positive and negative charges collect on each conductor. If the polarity of the voltage is reversed, then the charges also reverse. Capacitive sensors use an alternating voltage which causes the charges to continually reverse their positions. This charge motion generates an alternating electric current which is detected by the sensor. The amount of current flow is determined by the capacitance, which depends on the surface area of the conductors, the distance between them, and the dielectric constant of the material between them (such as air). The capacitance, C, is directly proportional to the surface area, A, and inversely proportional to the distance, d, between them. A larger surface area and smaller distance produces a larger current. For two parallel plate conductors, the capacitance is given by:

$$C = \varepsilon_r \varepsilon_0 \frac{A}{d}, \tag{10}$$

where ε_r is the dielectric constant (or static relative permittivity) and ε_0 is the electric constant (or vacuum permittivity). The value of the dielectric constant is 1 in vacuum and the electric constant is $8.854187817\ldots \times 10^{-12}$ A s/(V m).

Typically, the probe is one of the conductors and the measurement target is the other. If the sizes of the sensor and the target and dielectric constant of the material between them are assumed to be constant, then any change in capacitance is due to a change in the distance between the probe and the target [3].

Accelerometers for structural vibration measurement typically use the piezoelectric effect to generate a voltage signal that is proportional to acceleration. An accelerometer includes, at minimum, a seismic mass, piezoelectric material, and package that is connected to the structure under test. The piezoelectric material may be quartz, tourmaline, barium titanate, or lead zirconate titanate, or PZT, and produces a charge when strained by the inertial force applied by the mass during motion of the package. The corresponding voltage is equal to this charge divided by the piezoelectric material's capacitance. The output voltage is proportional to the inertial force and, therefore, the acceleration.

3. Experimental setup

In this study, the effect of a time delay in a capacitive sensor (relative to a piezoelectric accelerometer) was measured. The two transducers were used to measure the vibration of an oscillating target. The target was vibrated sinusoidally using a modal shaker (TIRAvib 51075) capable of generating oscillations up to 5000 Hz. A function generator (Hewlett Packard 33120A) was used to drive the shaker at the desired fixed frequency. The target motion was measured using both a low-mass accelerometer (PCB 352C23) and a capacitive sensor (Lion Precision C23B). The capacitive sensor signal

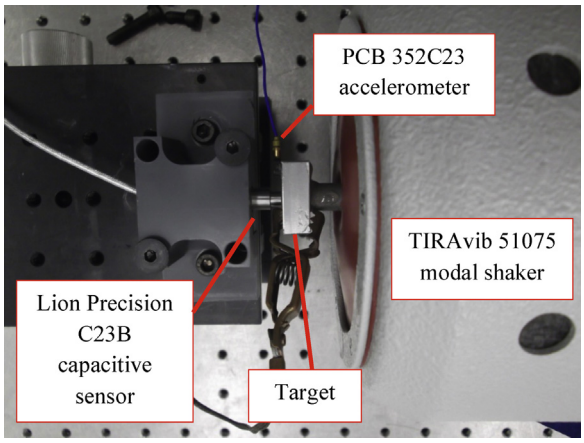

Fig. 6. Photograph (top view) of experimental setup.

was amplified using a Lion Precision CPL 290 Elite series amplifier. The amplifier bandwidth was set to 15 kHz. Data for both sensors was simultaneously acquired at 100 kHz using an NI data acquisition (DAQ) card. Fig. 5 shows a schematic representation of the measurement setup. A photograph is provided in Fig. 6.

Measurements were conducted over a frequency range of 100–5000 Hz. The measured data was digitally filtered using a 3rd order bandpass filter with a bandwidth of 100 Hz centered at the oscillation frequency. An example measurement result for 3000 Hz is provided in Fig. 7. A constant time delay between the accelerometer and capacitive sensor signals is observed. Fig. 8 shows the measured phase error (due to the time delay) as a function of the oscillation frequency. Within the measured bandwidth, the phase error varied linearly with frequency at a rate of −12.9 deg/kHz, which is consistent with the manufacturer-reported value [4]. Scatter from the linear best fit in the 1000–2000 Hz and 4000–4500 Hz ranges is suggested to be due to compliance in the wax interface between the accelerometer and target.

4. Phase correction algorithm

Given the frequency-dependent phase error for the capacitive sensor (Fig. 8), the effect of the time delay can be removed from the measured FRF. The measured phase, ϕ_m, is corrected by subtracting the phase error, $\Delta\phi$, which is determined from the product of the slope, S, from Fig. 8, (deg/Hz), and the frequency, f (Hz). See Eq. (11), where ϕ_c is the corrected phase.

$$\phi_c(f) = \phi_m - \Delta\phi = \phi_m - Sf \tag{11}$$

The real and imaginary parts of the measured FRF are then corrected using ϕ_c. See Eqs. (12) and (13), where it is assumed that the FRF magnitude is not affected by the time delay. Note that this approach is equivalent to multiplying the measured signal by $e^{i\omega\tau}$ in the frequency domain,[2] where τ is the time delay. However, knowledge of the time delay value is not required for the method described here. Additionally, Eq. (11) can be modified to incorporate nonlinearities in the measured phase.

$$Re\left(\frac{X}{F}(f)\right)_c = \left|\frac{X}{F}(f)\right| \cos(\phi_c(f)) \tag{12}$$

$$Im\left(\frac{X}{F}(f)\right)_c = \left|\frac{X}{F}(f)\right| \sin(\phi_c(f)) \tag{13}$$

To demonstrate the correction algorithm, FRF tests were performed on a cylindrical artifact (a modified boring bar blank) mounted in the spindle of a Haas TM-1 CNC vertical machining center (CAT-40 interface). A modally-tuned hammer (PCB 086C04) was used to excite the structure and the response was measured at the free end of the artifact using both the capacitive sensor and accelerometer.

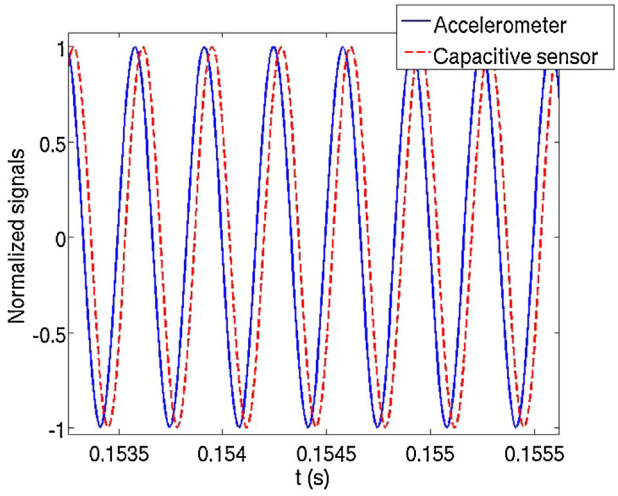

Fig. 7. Example measurement results for 3000 Hz excitation frequency.

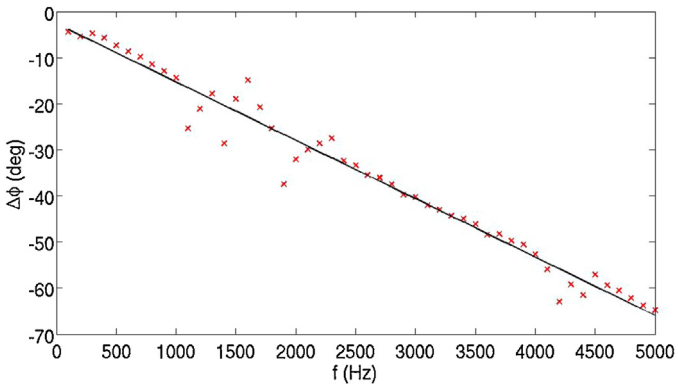

Fig. 8. Phase error between accelerometer and capacitive sensor. The best fit slope is −12.9 deg/kHz.

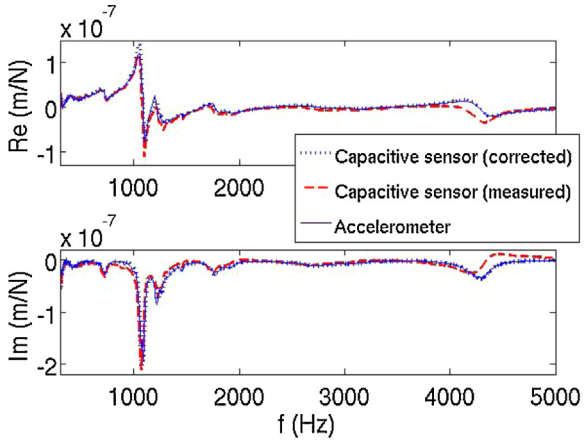

Fig. 9. Comparison between accelerometer and capacitive sensor FRFs. The corrected capacitive sensor result matches the accelerometer result.

[2] This is a non-causal operation, but would be performed as a post-processing step.

The data for all three sensors was acquired simultaneously at a 100 kHz sampling rate using the NI data acquisition device.

Fig. 9 shows the measured and corrected FRFs obtained using the capacitive sensor. Note that the uncorrected capacitive sensor measurement deviates from the accelerometer FRF at higher frequencies. In particular, for the mode near 4300 Hz in the uncorrected capacitive sensor FRF, the measured (dashed line) real part resembles the imaginary part of an error-free mode and the imaginary part resembles the inverted real part of an error-free mode. Smaller differences are also observed for the lower frequency modes. However, the corrected capacitive sensor result (dotted line) matches the accelerometer result (solid line).

5. Conclusions

In this study, the frequency-dependent phase error induced by a time delay is analyzed. It is shown for an example capacitive sensor system that, provided the phase error is measured, its effect can be removed in a post-processing step. A frequency domain correction algorithm is demonstrated for FRF measurements completed on a milling spindle-cylindrical artifact setup. The measurements show that the corrected FRF measured using the capacitive sensor agrees with the FRF measured using the piezoelectric accelerometer.

References

[1] Ewins DJ. Modal testing: theory. practice and application. 2nd ed. Hertfordshire: Research Studies Press LTD; 2000.
[2] Schmitz T, Smith KS. Mechanical vibrations: modeling and measurement. New York: Springer; 2012.
[3] http://www.lionprecision.com/tech-library/technotes/cap-0020-sensor-theory.html
[4] Lion Precision, TechNote LT03-0031 EliteSeries Amplitude/Phase Frequency Response, 2011.